I-V characteristics and nonclassical behavior in networks of small metal clusters

H. Zhang, D. Mautes, and U. Hartmann
Institute of Experimental Physics, University of Saarbruecken, P. O. Box 151150, D-66041 Saarbruecken, Germany
e-mail: h.zhang@mx.uni-saarland.de

INTRUDUCTION

The miniaturization of electronic components approaches the limit at which the functionality of the components cannot be described solely by classical physics. Quantum phenomena, such as electron tunneling, play an important role for devices with functional structures at the nanometer scale. For an investigation of the electron-transport in such small structures scanning tunneling microscopy (STM) and spectroscopy provide an ideal access..

EXPERIMENT

In this work monolayers of metal clusters of type $Au_{55}[P(C_6H_5)_3]_{12}Cl_6$, deposited on highly oriented pyrolytic graphite (HOPG) or Au(111) substrates were investigated with a low-temperature ultrahigh vacuum scanning tunneling microscope. The diameter of the cluster core is 1.4 nm. The ligand shell $[P(C_6H_5)_3]_{12}Cl_6$ has a thickness of about 0.35 nm. It acts as dielectric spacer. Apart from the usual charge-quantization phenomena, such as Coulomb blockade and staircase, negative differential resistance (NDR) was observed by performing *I-V* measurements at distinct locations on the cluster layers (see Fig. 1).

DISCUSSION

Surprising at first sight is the appearance of NDR if the tip is fairly close to a neighboring cluster (Fig. 1(c)). It is obvious that in this case one cannot neglect the capacitance between the tip and the neighboring cluster. This stray capacitance can evidently cause a significant change of the electrical potential of the neighboring cluster during the variation of the tunneling voltage which is applied between STM tip and substrate. The potential variation of the neighboring cluster in turn influences the potential of the primary cluster through the capacitance between the two clusters. That leads to a Coulomb blockade in the main current path. The neighboring cluster ultimately acts as a "gate".

SIMULATION

We performed a modeling of the resulting *I-V* curve using a Monte-Carlo method [1] based on the orthodox single-electron tunneling theory. A scheme of the corresponding cluster arrangement and the ersatz circuit together with the calculated behavior is shown in Fig. 2. In the case of Fig. 2(b) we found that NDR can only occur if the capacitance between the two neighboring clusters is larger than that between cluster and substrate. This situation is excluded in a treatment according to classical physics: The separation between the clusters (~ 7 Å) is larger than that between cluster and substrate (~ 3.5 Å).

We explain this phenomenon by a nonclassical capacitive behavior: For tunnel junctions electrons can overcome the dielectric or vacuum region through tunneling and this leads to a reduction in capacitance. As a consequence, the capacitance decreases with decreasing separation of the electrodes because the tunneling current increases.

Accordingly, we have chosen the proper values of capacitances and resistances for simulating all three cases. The results are in good agreement with the experimental findings.

ACKNOWLEDGEMENT

This work is supported by the Deutsche Forschungsgemeinschaft .

REFERENCES

[1] Ch. Wasshuber, H. Kosina and S. Selberherr, IEEE Transactions on Computer- Aided Design of Integrated Circuits and Systems **16,** 937 (1997).

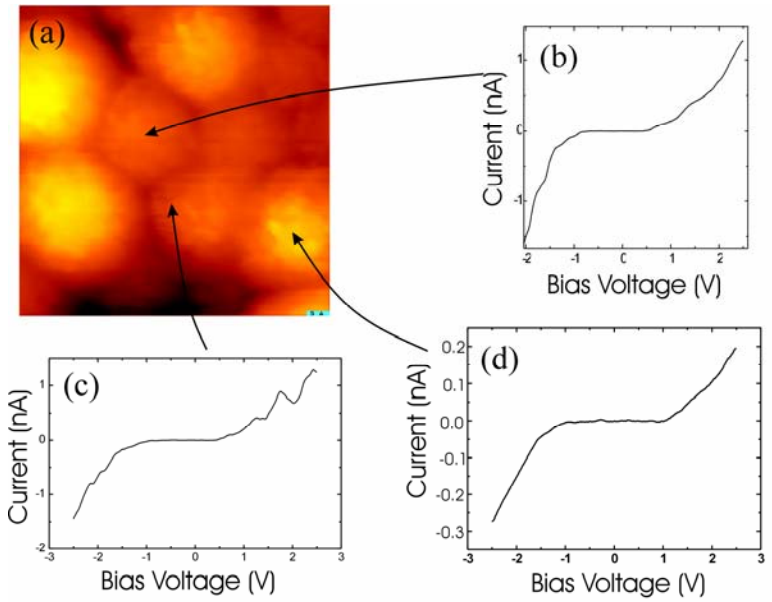

Fig. 1. (a) STM image of $Au_{55}[P(C_6H_5)_3]_{12}Cl_6$ clusters deposited on HOPG, obtained at a bias of 2 V and a current of 100 pA at a scan range of 7 nm x 7 nm. (b) *I-V* curve acquired above the center of a cluster, (c) away from the center and near a neighboring cluster, and (d) above a cluster which belongs to the second cluster layer, as marked in (a). Setpoint for (b) and (c): I_T = 0.7 nA, V_T = 2 V, for (d): I_T = 0.1 nA, V_T = 2V

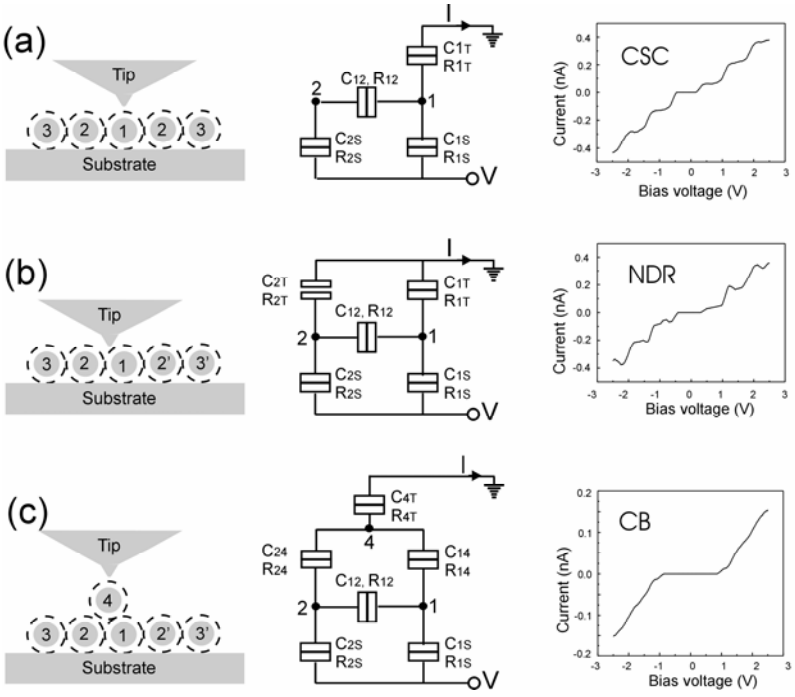

Fig. 2. Schematic diagrams of the different tip-cluster-substrate arrangements, the equivalent electrical circuits, and Monte-Carlo simulation of *I-V* curves. (a), (b) and (c) correspond to the cases of (b), (c) and (d) in Fig. 1, respectively. The C and R values chosen for modeling are: (a) C_{1T} = 0.2 aF, $C_{1S} = C_{2S}$ = 0.05 aF, C_{12} = 0.25 aF, R_{1T} = 5 GΩ, $R_{1S} = R_{2S}$ = 100 MΩ, R_{12} = 100 GΩ; (b) C_{1T} = 0.08 aF, $C_{1S} = C_{2S}$ = 0.03 aF, C_{12} = 0.25 aF, C_{2T} = 0.12 aF, R_{1T} = 5 GΩ, $R_{1S} = R_{2S}$ = 100 MΩ, R_{12} = 100 GΩ, R_{2T} = 1200 GΩ; (c) C_{4T} = 0.08 aF, $C_{1S} = C_{2S}$ = 0.05 aF, C_{12} = 0.25 aF, C_{14} = 0.25 aF, C_{24} = 0.27 aF, R_{4T} = 2 GΩ, $R_{1S} = R_{2S}$ = 200 MΩ, R_{12} = 100 GΩ, R_{14} = 8 GΩ, R_{24} = 80 GΩ